Heliyon 11 (2025) e41320

Contents lists available at ScienceDirect

Heliyon

journal homepage: www.cell.com/heliyon

Research article

Visible light induced photocatalytic degradation of norfloxacin using xC-TiO_2

Adnan [a,*,1], Kalsoom [a,1], Farah Muhammad Zada [a], Sarwat [a], Ho Soonmin [b], Behramand Khan [c], Muhammad Alamzeb [d], Wei Sun [e], Jawad Ikram [a], Najeeb ur Rehman [a]

[a] Institute of Chemical Sciences, University of Swat, Swat, 19120, Khyber Pakhtunkhwa, Pakistan
[b] Faculty of Health and Life Sciences, INTI International University, Putra Nilai, 71800, Negeri Sembilan, Malaysia
[c] Department of Chemistry, Islamia College University, Peshawar, 25120, Pakistan
[d] Department of Chemistry, University of Kotli, Kotli, 11100, Azad Jammu & Kashmir, Pakistan
[e] College of Chemistry and Chemical Engineering, Hainan Normal University, Haikou, 571158, China

ARTICLE INFO

Keywords:
Visible light photocatalysis
Norfloxacin degradation
Carbon-doped TiO_2
Antibiotic removal
Nanoparticles
Kinetics
Isotherm
Pollution and wastewater treatment

ABSTRACT

In recent years, antibiotic pollution has become a major environmental concern. The extensive production and widespread use of prescribed antibiotics have significantly impacted ecosystems. The main objective of the present study is to investigate the photocatalytic degradation of the antibiotic norfloxacin (NFX) under visible light. In this work photocatalysis of NFX was demonstrated under the source of visible radiation by using carbon dopped-titania (**C-TiO_2**) nanoparticles as catalyst prepared by a modified sol-gel method using n-hexane and benzene as carbon precursors. The synthesized samples were characterized by scanning electron microscopy (SEM), X-ray diffraction (XRD), and energy dispersive X-ray (EDX) techniques. The effect of various parameters like initial concentration, catalyst dosage, irradiation time, pH, and inorganic ions were investigated on the photocatalysis of NFX. The XRD and SEM analysis exhibits that the synthesized **C-TiO_2** nanoparticles were of anatase phase having spherical shape with a mean particle size of about 11–17 nm. The results shows that the best photocatalytic efficiency (74 % & 81 %) was achieved at pH = 8 in 150 min. The degradation of NFX follows pseudo-2nd -order kinetics, while favors Langmuir isotherm model. The inhibition effect of various inorganic ions on the photocatalysis of NFX was in the order of $F^- > SO_4^{2-} > HCO_3^- > NO_3^-$. The present study shows that **C-TiO_2** is an optimistic and efficient catalyst for the photocatalysis of NFX antibiotics.

1. Introduction

Recently personal care products and pharmaceuticals have gained much attention due to their ubiquitous use and its flux to aquatic media [1]. Among them, antibiotics are more widely used nowadays. The main sources of antibiotics in the aqueous system are the pharmaceutical industry [2], pesticides, veterinary drugs and medicines [3].

The presence of antibiotics in an aquatic ecosystem is of particular concern because their presence in small quantities may pose

* Corresponding author.
E-mail addresses: adnanchem@yahoo.com, adnanchem@uswat.edu.pk (Adnan).
[1] Adnan and Kalsoom contributed equally to this work and share first authorship.

https://doi.org/10.1016/j.heliyon.2024.e41320
Received 30 August 2024; Received in revised form 27 November 2024; Accepted 17 December 2024
Available online 21 December 2024

antibiotic resistance to microorganisms, and adversely affects marine and land life. Norfloxacin (NFX) is a synthetic [4] second-generation fluoroquinolone antibiotic prescribed for treating bacterial infections in humans and animals [3]. It has mostly been detected in different resources of water like ground, surface, drinking and seawater. Moreover, it is also ranged in other environmental effluents due to nominal biodegradation and low metabolic rate of NFX [5,6]. About 75 % of NFX is excreted from the body in pharmacologically active form [7].

Various methods such as photolysis [8], membrane filtration [9], precipitation [10], adsorption [11–13], advanced oxidation [14], ozonation [15], and photocatalysis, have been employed for the removal of NFX from water because NFX cannot be degraded completely by natural process [16]. Therefore, it is still necessary to devise a facile method for the removal of NFX from water that is efficient and environmentally friendly. Among these techniques, photocatalysis shows high efficiency in the elimination of antibiotics from water [17–19] due to low cost, long-lasting stability, and ability to reduce the incomplete degradation of NFX and completely degrade the pollutants into CO_2 and H_2O [20].

In the past decade, researchers have used different catalysts for the complete degradation of NFX i.e., Ding, D et al. [21],synthesized magnetic nanoparticles through a simple method for persulfate activation to degrade norfloxacin antibiotic. About 90 % of norfloxacin was degraded by this method only in 60 min, Ma, X et al. [22], used commercial zerovalent nanoparticles to activate hydrogen peroxide for the degradation of norfloxacin under ultrasonic irradiation. Norfloxacin was completely removed in 30 min by this method. Mohan, H et al. [23], synthesized nanocomposite of iron oxide and titania via a sol-gel method to degrade norfloxacin under visible light. The result showed that the composites take only 60 min for the complete degradation of norfloxacin. Lv, X et al. [19], synthesized copper-dopped bismuth oxybromide by solvothermal method for the degradation of norfloxacin under visible light. The synthesized catalyst retained 95 % of its catalytic activity after being used five times. Cao, D et al. [24], degraded norfloxacin photo electrocatalytically by using electrodes made from the composite of Ag_3PO_4 and $BiVO_4$ under visible light. By this process 5 mg/L, norfloxacin takes only 90 min to degrade completely.

Many catalysts have been synthesized and utilized till now but titanium dioxide (TiO_2) is still widely used as a photocatalyst that is economical, most abundant, nontoxic, chemically more stable and shows high photo reactivity under ultraviolet light(5–9% of solar light) at shorter wavelength i.e. $>$ 387 nm [25]. However, the use of TiO_2 materials as a photocatalyst is significantly hindered by their largest band gap of 3.0–3.2 eV, the short life span of photo-generated electron-hole-pair, and low photonic efficiency [26]. Many attempts have been made to shift the photocatalytic activity of TiO_2 to the visible region of the spectrum by doping the surface of TiO_2 with transition metals, anionic nonmetals, and anchoring organic dye on its surface [27,28] which will reduce the bandgap from ultraviolet to visible part of the spectrum. Among the various dopant used, carbon-doped TiO_2 has gained considerable attention due to its high absorption coefficient and narrow band gap. Carbon doping provides a carboxyl group that acts as an anchoring group for the photocatalyst. The utilization of light is extended by carbon doping and TiO_2 is activated by affecting the electronic environment of both Ti cations and O anions. Recently it has been found that the life-span and carrying capacity is increased with carbon doping [29, 30].

In this study carbon doped titania (**C-TiO_2**) synthesized by the sol-gel method using n-hexane and benzene as precursors of carbon. To our best study, this is the first time to synthesize **C-TiO_2** by this method and used for the degradation of NFX. We have conducted this study to analyze the effect of different parameters including catalyst dosage, initial concentration, irradiation time, pH, and various inorganic ions on the photocatalytic degradation of NFX. To analyze the rate of degradation various kinetic and isothermal models were applied and to investigate the feasibility of the degradation process and degradation equilibria were conducted.

2. Experimental

2.1. Chemicals and reagents

The chemicals employed to conduct this research were of analytical grade. Titanium tetrachloride ($TiCl_4$, 99 %), boric acid (H_3BO_4, 99 %), sodium nitrate ($NaNO_3$), sodium fluoride (NaF), sodium bicarbonate ($NaHCO_3$), and sodium sulfate (Na_2SO_4) were purchased from Deajung, Korea. Ethanol (C_2H_5OH, 99 %) and phosphoric acid (H_3PO_4, 85 %) were supplied by BDH Laboratory Supplies, Poole, England. Benzene (C_6H_6, Extra pure), hydrochloric acid (HCl, 37 %), and sodium hydroxide (NaOH, pellets) purchased from Merck, Germany. Acetic acid (CH_3COOH, 100 %) and n-hexane (C_6H_{14} extra pure) purchased from Sigma-Aldrich, Germany. Standard norfloxacin (NFX) antibiotic obtained from Shaheen Pharmaceutical Industry, Swat, Pakistan on request. Distilled water supplied by ICS University of Swat. An aluminum foil is used to wrap the solution and reagents to prevent the entrance of any contaminant and or light.

2.2. Synthesis of carbon doped titania (C-TiO_2) photocatalysts

C-TiO_2 nanoparticles were prepared by modified sol-gel method [31] using two different carbon precursors i.e., for sample A; n-hexane and for sample B; benzene was used as a source of carbon under the same conditions.

First of all, 300 ml ethanol taken in a conical flask (500 ml) and 0.2 mol of ice cold $TiCl_4$ was added to it dropwise with the help of a dropping funnel under vigorous stirring using a magnetic stirrer. After stirring for 80 min, a transparent yellowish sol was formed. In the case of sample A; 40 ml of n-hexane was added, while in the case of sample B; 35 ml of benzene was added to the sol and stirred for about 20 h (at room temperature) until the sol become colorless. The sol then heated at 100 °C and maintained at this temperature for 5 h. After heating the sol converted into yellowish gel. The gel then dried in the oven and grinded into a fine powder with the help of a pestle and mortar. The gel was calcined for 5 h at 500 °C in the furnace, **C-TiO_2** in the form of yellowish powder obtained. The obtained

powder was washed with distilled water and then dried to remove moisture.

The **C-TiO_2** was termed **nC-TiO_2** and **bC-TiO_2**. Where "n" stands for n-hexane and "b" stands for benzene as carbon source/precursor. The powdered samples were then stored in an airtight container for further studies.

The flow diagram for the synthesis of **nC-TiO_2** and **bC-TiO_2** is given in Fig. 1.

2.3. Characterization

2.3.1. X-ray diffraction (XRD)

X-ray diffractometer Model No. D8, Advance Bruker Company, Germany was used to examine the structure and phase of the synthesized catalyst. This analysis was accomplished in the range of $2\theta = 10°–70°$ using X-rays (Cu Kα radiation) of wavelength 1.5418 A° (0.15418 nm), at a scan rate of 1.2° per minute using 40 kV accelerating voltage and 30 mA emission current. The mean crystallite size was determined by Scherrer's formula.

2.3.2. Scanning electron microscopy (SEM)

Scanning electron microscope (SEM), Jeol (JSM6490, Tokyo, Japan) was used to evaluate the surface morphology and size of **C-TiO_2** nanoparticles by using a beam of electrons and to give high resolution images of the samples.

2.3.3. EDX (energy dispersive X-ray)

To check the chemical/elemental composition of the nano-crystalline powder SEM-EDX analysis was performed using (EDX, JSM5910, JEOL, Japan).

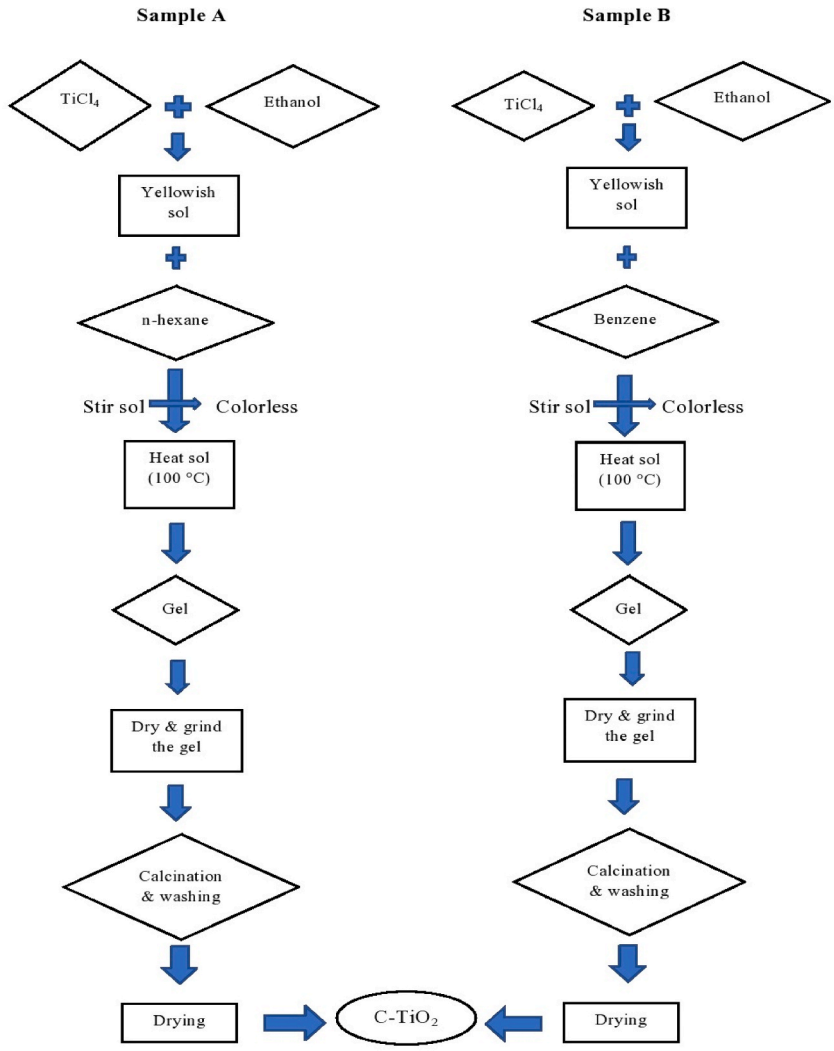

Fig. 1. Flow diagram for the synthesis of **C-TiO_2** nanoparticles.

2.4. Photocatalytic degradation studies of NFX

To degrade NFX antibiotics by C-TiO_2 nanoparticles using visible radiation, working solutions in the range of 10–50 ppm were used. First of all, a microreactor was set off in the lab shown in Fig. 2. For the degradation process 25 ml solution was taken in 100 ml beaker with the addition of a different amount of **C-TiO_2** nanoparticles from 5 to 30 mg. Then the mixture was stirred for 30 min in dark to attain adsorption-desorption equilibrium. After stirring in dark the mixture was exposed to a visible lamp (500-W linear halogen lamp) at a distance of 15 cm for a fixed interval of time with constant stirring.

The molar absorptivity coefficient (ε) of NFX at 270 nm was determined as 3025 L mol^{-1} cm^{-1} in a solution of initial concentration prior to photocatalytic degradation. This value was used as a reference for calculating NFX concentration over the course of the degradation experiments. After degradation, the sample was taken and centrifuged for 15 min to separate the catalyst from the sample, then the sample was filtered through a nylon membrane filter to remove any nanoparticles. The sample was then quantitatively analyzed by a single beam spectrophotometer (Biotechnology Medical Services (BMS), K. Canada Inc) at the λ_{max}. of NFX (270 nm). The % degradation of NFX under visible light was calculated by using equation 1.

$$\%\text{degradation} = \frac{C_i - C_e}{C_i} \times 100 \quad (1)$$

C_i and C_e represent the concentration of solution before and after degradation, respectively.

3. Result and discussion

3.1. Characterization

3.1.1. XRD

XRD analysis was performed to investigate the structure and crystallinity of the synthesized **C-TiO_2** photocatalysts. Fig. 3 shows the XRD patterns of **nC-TiO_2** and **bC-TiO_2** in the region of 2 θ = 10–70°. The main diffraction peaks detected in the XRD pattern for **nC-TiO_2** at 25.46°, 37.95°, 48.20°, 54.03°, 55.2°, and 62.94° and for **bC-TiO_2** at 25.37°, 37.93°, 48.12°, 54.03°, 55.19°, and 62.82° corresponded to (101), (004), (200), (105), (211) and (204) crystal planes indicates that both samples are of pure anatase phases which were in agreement with JCPDS card No. (21–1272) [32,33] and (01-073-1764) [34].

The average crystallite size was determined from the XRD plot by using the Debye-Scherrer formula given in equation (2),

$$D = K\lambda/(\beta \cos\theta) \quad (2)$$

Here "*D*" represents the size of crystallite (nm), "*K*" is Scherrer constant whose value is approximately 0.9, "β" is FWHM (Full width at half maximum) in radians, "λ" is the wavelength of X-ray used (0.15418 nm) and "θ" is the peak position in radian. The average size calculated was 11.3 nm for **nC-TiO_2** and 17.8 nm for **bC-TiO_2** nanoparticles.

3.1.2. SEM

To analyze the particle size and surface morphology of the synthesized photocatalyst SEM studies were performed. Fig. 4a, b, c,and d shows the SEM images of both samples (**nC-TiO_2** & **bC-TiO_2**). It clarifies from the respected figure that both the samples are made up of nanoparticles that are spherical shaped and the particles are mostly agglomerated. The size of the particles ranges from 6 to 15 nm with an average particle size of 10.9 nm for **nC-TiO_2** and from 11 to 19 nm for **bC-TiO_2** with an average particle size of 15.7 nm which are in close agreement with 11.3 nm and 17.8 nm calculated by Scherrer's formula. The particle are assembled into aggregated form having size ranges from 0.357 to 0.948 μm for **nC-TiO_2** and from 0.299 to 0.587 μm for **bC-TiO_2**.

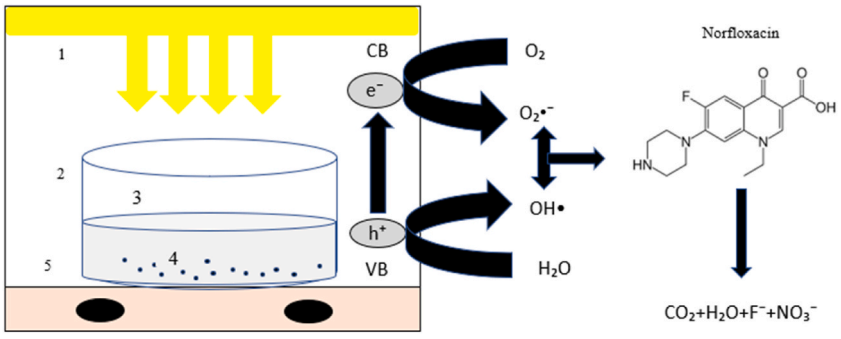

Fig. 2. Microreactor assembly for photocatalytic degradation of NFX (**1**. visible light - 500-W linear halogen lamp, **2.** Sample container, **3.** NFX solution, **4. C-TiO_2** nanoparticles, **5.** Magnetic heating stirrer).

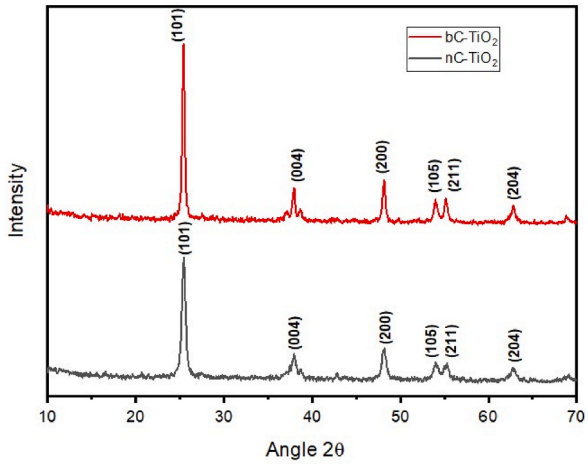

Fig. 3. XRD patterns of nC-TiO_2 and bC-TiO_2.

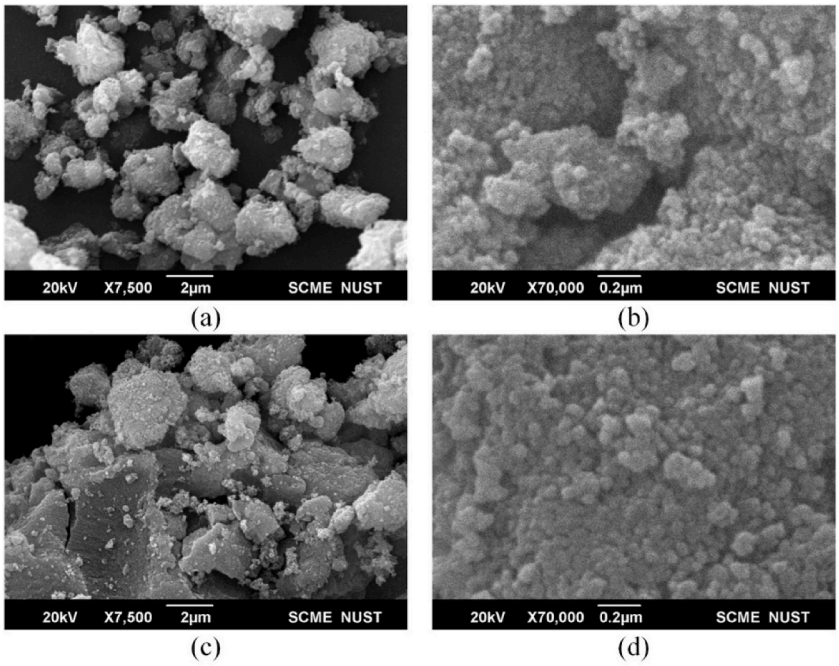

Fig. 4. SEM images (a) × 7500 magnifications of **nC-TiO_2** (b) × 70,000 magnifications of **nC-TiO_2** (c) × 7500 magnifications of **bC-TiO_2** and (d) × 70,000 magnifications of **bC-TiO_2** nanoparticles.

3.1.3. SEM-EDX

SEM-EDX analysis was performed to check the elemental composition of the nanocrystalline powder. The EDX spectrum shown in Fig. 5a and b indicates the presence of carbon in addition to titanium and oxygen. The elemental composition given in Table 1 indicates that the atomic %age of carbon is 6.24 % in **nC-TiO_2** and 7.98 % in **bC-TiO_2**.

3.2. Optimization of various parameters using C-TiO_2 nanoparticles

3.2.1. Effect of irradiation time

The influence of irradiation time on the photocatalytic degradation of NFX using both the samples of **C-TiO_2** was studied for various irradiation time i.e., 30, 60, 90, 120, and 150 min under visible light using other parameters constant i.e., initial concentration (10 ppm), photocatalyst dosage(10 mg) and pH 1. Fig. 6 reveals that the %photodegradation was increased and the amount of NFX in the solution was decreased when the time of irradiation was extended. This is because as the irradiation time increases the NFX molecules

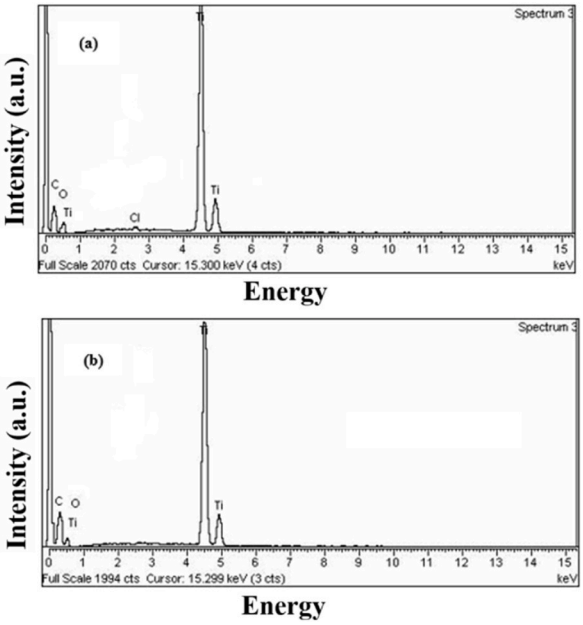

Fig. 5. EDX spectrum (a) **nC-TiO_2** (b) **bC-TiO_2**.

Table 1
Elemental composition of **nC-TiO_2** and **bC-TiO_2**.

Element	nC-TiO_2		bC-TiO_2	
	Weight %	Atomic %	Weight %	Atomic %
O	22.83	46.92	19.62	42.22
C	9.08	6.24	11.1	7.98
Ti	67.6	46.39	69.28	49.8
Cl	0.49	0.45	0.00	0.00
Totals	**100**	**100**	**100**	**100**

will have sufficient time to be adsorbed on the active sites of the photocatalyst nanoparticles (**C-TiO_2**) which led to enhanced degradation [35]. Furthermore, more radiation is also responsible for the decrease of NFX concentration in the solution. The best result was shown at 150 min i.e., 71 % for **nC-TiO_2** and 62 % **bC-TiO_2**. After 150 min equilibrium was attained between adsorption and

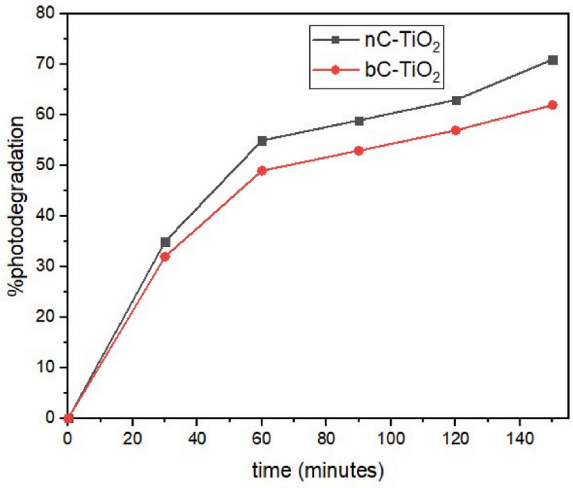

Fig. 6. Effect of irradiation time on the %photodegradation of NFX (experimental conditions: 10 ppm NFX solution, 10 mg photocatalysts, and pH 1).

photodegradation [36].

3.2.2. Effect of catalyst dosage

The process of photocatalytic degradation influenced by catalyst dosage. Increasing the photocatalyst dosage up to a certain limit will increase the %photodegradation due to the elevation of surface active sites of photocatalyst and hence $OH^{\bullet}$ involved in the photocatalytic degradation [37]. To analyze the effect of the amount of **C-TiO_2** nanoparticles (photocatalyst) on the degradation of NFX, the photocatalysts were taken in different amounts ranging from 5 to 30 mg/25 ml i.e., 5, 10, 15, 20, and 30 mg keeping other parameters constant i.e., initial concentration (10 ppm), irradiation time (150 min) and pH 1. Fig. 7 shows the effect of catalyst dosage (**nC-TiO_2** and **bC-TiO_2**) on photocatalytic degradation of NFX. It was observed that with the increase in the amount of **nC-TiO_2** from 5 mg to 10 mg and **bC-TiO_2** from 5 mg to 15 mg the % photodegradation of NFX also increases, due to enrichment of reactive sites which increase the formation of radicals. The maximum photodegradation observed was 71 % for **nC-TiO_2** and 77 % for **bC-TiO_2**. However, when the catalyst dosage was further increased to 30 mg, the photodegradation declined significantly from 71 % to 42 % for **nC-TiO_2** and from 77 % to 67.9 % by using **bC-TiO_2**. The reason for such a drop is the turbidity of a solution by aggregation of **C-TiO_2** photocatalysts which decreases the penetration power of light and so less amount of light will enter the solution and the rate of the photocatalytic process decreases notably [23,38].

3.2.3. Effect of initial concentration of NFX

The crucial factor in photocatalytic degradation is the initial concentration of the substrate. Commonly the rate of a chemical reaction increases with an increase in the concentration of reactants to some limit and then decreases [39]. To investigate the effect of initial concentration on the photocatalytic degradation of NFX, solutions of different concentrations i.e., 10, 20, 30, 40, and 50 ppm were used keeping other parameters constant i.e. optimum time (150 min), optimum catalyst dosage 10 mg of **nC-TiO_2** and 15 mg of **bC-TiO_2**, and pH 1. Fig. 8 shows that the %photodegradation of NFX decreased from 71 to 25 % for **nC-TiO_2** and from 77 to 29.9 % for **bC-TiO_2** when the concentration of the solution was increased from 10 to 50 ppm. The decrease in %photodegradation is the consequence of dissolved NFX which scatter the light, reduce the penetration of light and cause saturation of the active sites of **C-TiO_2** photocatalysts by the adsorption of NFX which reduces the rate of production of e^{-}-H^{+} pair and $OH^{\bullet}$. At lower concentrations, the % photodegradation was high due to the presence of more free active sites and a low ratio between dissolved NFX and adsorbent sites [40].

3.2.4. Effect of pH

One of the important parameters affecting photocatalytic degradation is pH of the solution which significantly affects the degradation process of organic contaminants. To analyze the impact of pH on photocatalysis of NFX by **C-TiO_2** photocatalysts fixed amount of photocatalysts (10 mg of **nC-TiO_2** and 15 mg of **bC-TiO_2**) and an initial concentration of 10 ppm were used for each experiment. The degradation was checked from pH 2 to pH 10 for optimum time (150 min). The data obtained is represented graphically in Fig. 9. The result showed that pH strongly influences the degradation of NFX and the best photocatalytic activity is shown at weak alkaline condition pH (8) than acidic pH (2, 4, 6) and alkaline pH (9, 10). Changing pH affects the active sites of C-TiO_2 photocatalysts involved in the production of e^{-}-H^{+} pair and $OH^{\bullet}$. The generation of $OH^{\bullet}$ (strong oxidant) is easier in alkaline medium due to the presence of OH^{-} in excess [7]. The point of zero charges (PZC) for C-TiO_2 is reported at pH 5.5 [41]. So, the surface of C-TiO_2 nanoparticles was positive at pH less than 5.5 and a negative charge at pH above 5.5 [42,43]. On the other hand, NFX has two acid dissociation constants (pKa) at 6.1 and 8.6 [44]. Therefore, NFX sis positively charged at pH less than 6.1 due to protonation of carboxyl group, in zwitter ionic form between pH 6.1 and 8.6 due to deprotonation of carboxyl group only, and negatively charged at high pH due to deprotonation of amine group, and hence the degradation was retarded at alkaline conditions due to repulsion between **C-TiO_2** photocatalysts and NFX.

3.3. Kinetic models

In order to evaluate the rate of degradation and kinetics of NFX by **C-TiO_2** nanoparticles, two kinetic models pseudo 1st and 2nd

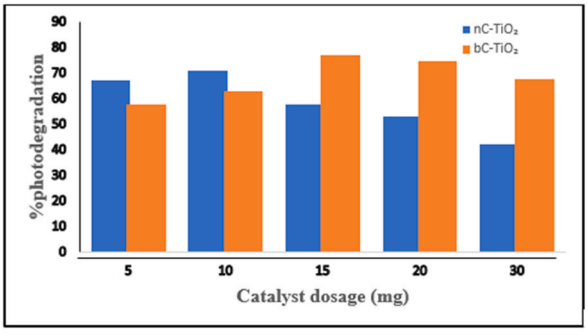

Fig. 7. Effect of catalyst dosage on %photodegradation of NFX (experimental conditions: 10 ppm NFX solution, irradiation time 150 min, and pH 1).

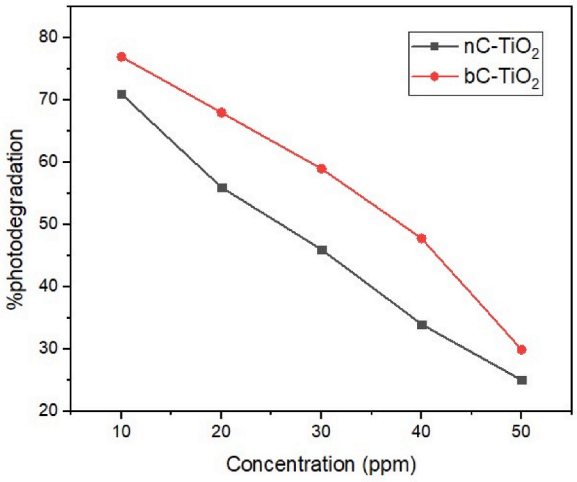

Fig. 8. Effect of initial concentration of NFX on %photodegradation of NFX (experimental conditions: irradiation time 150 min, 10 mg **nC-TiO$_2$**, 15 mg **bC-TiO$_2$** and pH 1).

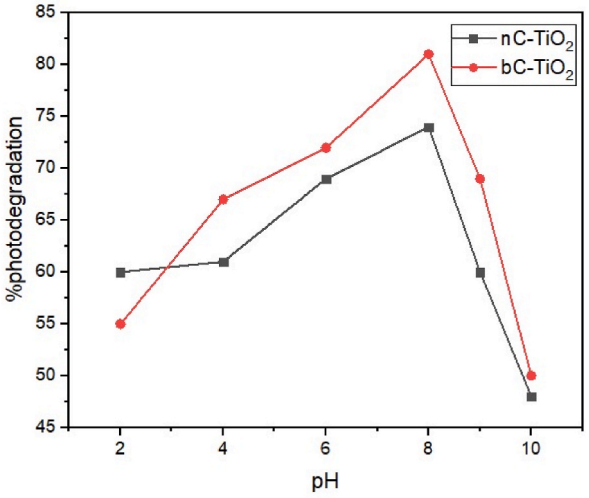

Fig. 9. Effect of pH on %photodegradation of NFX (experimental conditions: 10 ppm NFX solution, irradiation time 150 min, 10 mg **nC-TiO$_2$** and 15 mg **bC-TiO$_2$**).

order were used.

3.3.1. *Pseudo 1st order kinetic model*

The pseudo 1st order kinetic model was applied to obtained the data and the equation is given below in equations (3) and (4):

$$\log\left(q_e - q_t\right) = \frac{\log q_e - K_1 \times t}{2.303} \tag{3}$$

where

$$q_e \text{ or } q_t = \frac{C_i - C_e \times V}{m} \tag{4}$$

Here in equation (4) "q_e" represent the degradation capability at the optimal time, "q_t" represents the degradation at any time, "C_i" and "C_e" represent the initial and final concentration of NFX, "V" represents the volume of NFX solution used and "m" represents the mass of photocatalyst used for degradation of NFX.

While here K_1 represents the rate constant of pseudo 1st order KM (min^{-1}). Rate constant was determined from a plot between time (minutes) and log (q_e-q_t) Fig. 10a and b shows pseudo 1st order kinetics model plots for NFX using **nC-TiO$_2$** and **bC-TiO$_2$**.

Different values of parameters are tabulated and are given in Table 2 (values of R^2 and q_e cal. don't match q_e exp.) it is confirmed that pseudo 1st order KM is not appropriate for the photocatalytic degradation of NFX.

3.3.2. Pseudo 2nd order kinetic model

The mathematical relation for pseudo 2nd order kinetic model is given by equation (5):

$$\frac{t}{q_t}=\frac{t}{q_e}+\frac{1}{K_2 q_e^2} \tag{5}$$

The K_2 value (rate constant for 2nd order reaction) and q_e (equilibrium degradation) can be obtained from the value of intercept (C) and slope (m) of the graph between t (time) and t/q_t shown in Fig. 11a and b values of the different parameters are tabulated in Table 2 (value of R^2 and q_e cal. match q_e exp.) it is confirmed that photocatalytic degradation of NFX favors pseudo 2nd order kinetic model (see Fig. 12).

Here From Table 2 it is confirmed that photocatalytic degradation of NFX by both **nC-TiO$_2$** and **bC-TiO$_2$** follows pseudo-2nd order kinetic model.

3.4. Degradation equilibrium studies

To investigate the mechanism of adsorption and sorbent-sorbate equilibrium relationship [45] adsorption (equilibrium) isotherms were designed which play an important role in exploring the model appropriate for the proposed task. These isotherms explain how the contaminants and adsorbents interact [46,47]. Freundlich and Langmuir's isotherms were applied for degradation equilibrium studies.

3.4.1. Freundlich isotherm

Freundlich isotherm (FI) is used to study non-ideal degradation and to explain heterogenous surface degradation. The relation for FI is given in equation (6):

$$log\ q_e = log\ K_f + 1/n\ log\ C_e \tag{6}$$

In equation (6), q_e represents the equilibrium degradation, K_f represents the capacity of maximum degradation, C_e represents the equilibrium concentration whereas $^1/_n$ (slope) shows the extent of degradation, where n is the divergence from the intensity. A graph plotted between log q_e and log of C_e results in straight line having slope $^1/_n$ shown in Fig. 12 a &b

$$q_e=\frac{(C_i-C_e)V}{m} \tag{7}$$

To determine the value of q_e is shown in equation (7), where C_i represents the initial concentration of NFX, V is the volume of a sample taken, and m is the mass of **C-TiO$_2$** nanoparticles.

The values of various parameters tabulated in Table 2 indicate that the Freundlich isotherm model is not fit for the degradation of NFX by **C-TiO$_2$** nanoparticles.

3.4.2. Langmuir isotherm

Langmuir isotherm (LI) is one of the most extensively used for photocatalytic degradation. It assumes that during degradation the molecules are adhered in monolayer and uniformly on the photocatalyst surface and the molecules adsorbed in different locations have no interaction between. The following equation (8) is used for LI.

$$\frac{C_e}{q_e}=\frac{1}{k_L}+\frac{a_L}{k_L}\times C_e \tag{8}$$

In Equation No. 8, C_e represents the equilibrium concentration, q_e shows the amount of NFX degraded photo catalytically, k_L and a_L represent constants for Langmuir degradation isotherm, where k_L shows the highest photocatalytic degradation and a_L energy of bonding. The plot of C_e/q_e vs C_e will be used for calculating the k_L and a_L values from the intercept ($1/k_L$) and slope (a_L/k_L).

The values of various parameters given in Table 3 calculated from the plot of C_e/q_e vs C_e shown in Fig. 13a and b indicate that degradation of NFX by **C-TiO$_2$** nanoparticles Langmuir degradation isotherm.

The value of R^2 for Freundlich degradation isotherm comes out to be 0.74731 (**nC-TiO$_2$**) and 0.56942 (**bC-TiO$_2$**) and for Langmuir degradation isotherm 0.98216 (**nC-TiO$_2$**) and 0.95144 (**bC-TiO$_2$**) nanoparticles. The value of R^2 shows that the NFX degradation favors the Langmuir adsorption isotherm.

3.5. Effect of inorganic ions

To evaluate the influence of various inorganic ions (like SO_4^{2-}, HCO_3^-, NO_3^-, F^-) on the photocatalytic degradation of NFX, using optimized parameters i.e., amount of catalyst (10 mg for **nC-TiO$_2$** and 15 mg for **bC-TiO$_2$**), 25 ml of 10 ppm NFX solution, irradiation time 150 min and pH (8) were used. Fig. 14 shows that NO_3^- ions have no apparent effect on the degradation of NFX by virtue of the highest oxidation state of nitrogen (+5) and so are not involved in the consumption of holes or radicals. While SO_4^{2-}, HCO_3- and F^-

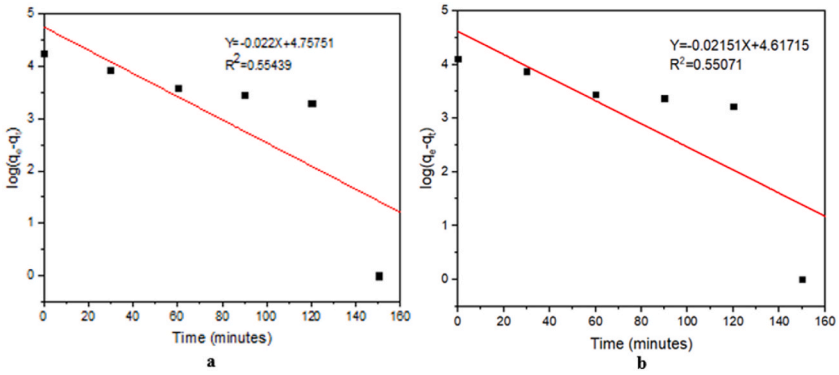

Fig. 10. Pseudo 1st order KM for NFX (a) **nC-TiO$_2$** (b) **bC-TiO$_2$** nanoparticle.

Table 2
Comparison of pseudo 1st and 2nd order kinetic models.

Pseudo 1st order KM			Pseudo 2nd order KM		
Parameter	nC-TiO_2	bC-TiO_2	Parameter	nC-TiO_2	bC-TiO_2
q_e exp (μg/g)	17732.5	12850	q_e exp.(μg/g)	17732.5	12850
q_e cal.(μg/g)	57215	41414.26	q_e cal.(μg/g)	18518	14285.7
K_1 (min^{-1})	5.0566×10^{-2}	4.95×10^{-2}	K_2 (g/μg min^{-1})	3.2×10^{-6}	2.98×10^{-6}
R^2	0.55439	0.55071	R^2	0.949	0.9037

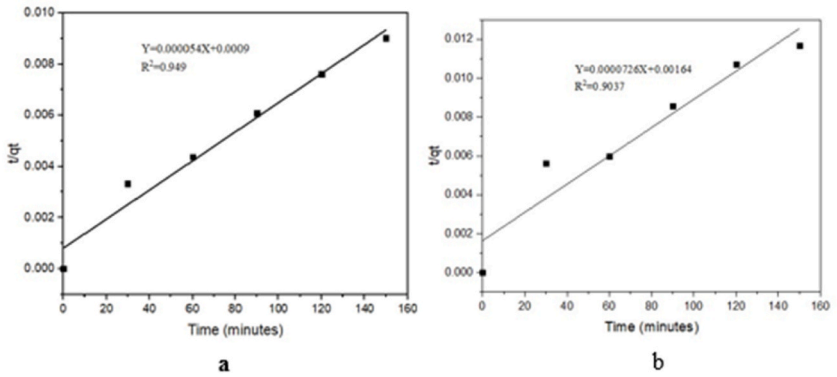

Fig. 11. Pseudo 2nd order KM plot for NFX using (a) **nC-TiO$_2$** (b) **bC-TiO$_2$** nanoparticles.

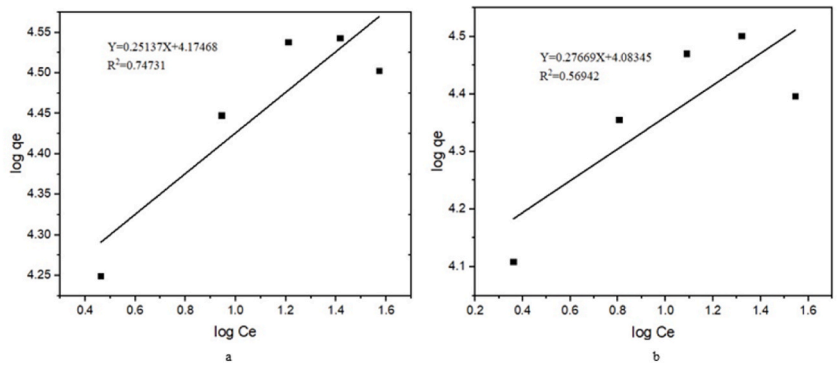

Fig. 12. Freundlich isotherm plot for NFX (a) **nC-TiO$_2$** (b) **bC-TiO$_2$** nanoparticles.

Table 3
Comparison of Freundlich and Langmuir degradation isotherms.

Freundlich isotherm			Langmuir isotherm		
	nC-TiO_2	bC-TiO_2		nC-TiO_2	bC-TiO_2
R^2	0.74731	0.56942	R^2	0.98216	0.95144
k_f	14951	12118	k_L	21739	53475
n	3.978	3.6141	a_L	0.608	1.978

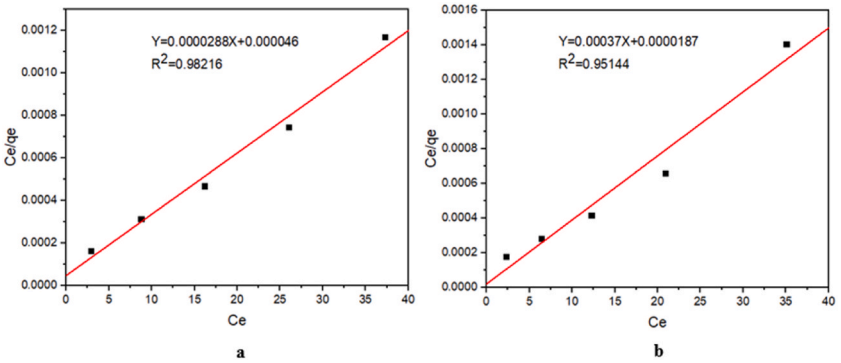

Fig. 13. Langmuir isotherm plot for NFX (a) **nC-TiO_2** (b) **bC-TiO_2** nanoparticles.

adversely affect the photocatalytic degradation of NFX because, both SO_4^{2-}, HCO_3^- ions are the scavengers of $OH^\bullet$ radical [3,48], and F^- suppress the degradation of NFX because of the hydrogen bond between OHF (OH——F) almost all over the **C-TiO_2** nanoparticles which would cause retardation of $OH^\bullet$ radicals formation as the OH^- ions become the part of the hydrogen bond.

3.6. *Effect of real water samples*

To analyze the impact of various samples of water on the photocatalytic degradation of NFX with both samples of **C-TiO_2**. Working solutions were prepared in water from various sources like river water (RW), tap water (TW), and distilled water (DW). The process was carried out using optimum parameters i.e., 10 ppm initial concentration, 10 mg of **nC-TiO_2** and 15 mg of **bC-TiO_2** of photocatalyst nanoparticles, 150 min irradiation time, and pH 8. Fig. 15 indicates the order of degradation of NFX i.e. DW > TW > RW. DW shows the best result due to the absence of microorganisms and organic matters, the moderate efficiency of TW is the result of limited organic matter and residual chlorine while RW shows the lowest degradation capability. The % photocatalytic degradation is in the range of 48–74 % (**nC-TiO_2**) and from 53 to 81 % **(bC-TiO_2)**. From the result, it is clear that river water significantly decreased the degradation of NFX antibiotic due to the presence of various interfering ions which are involved in the consumption of radicals and ions [49,50].

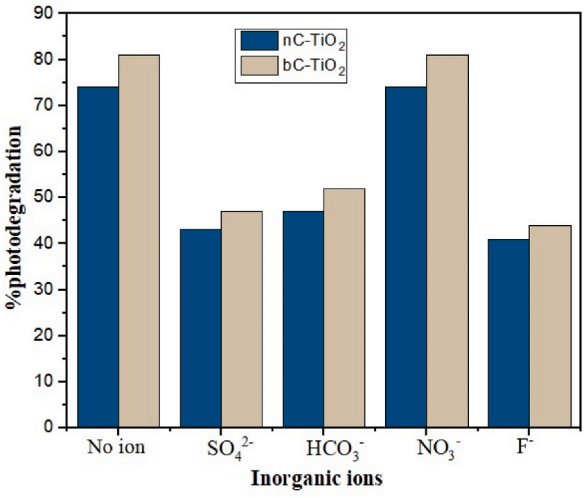

Fig. 14. Effect of inorganic ions on % photodegradation of NFX.

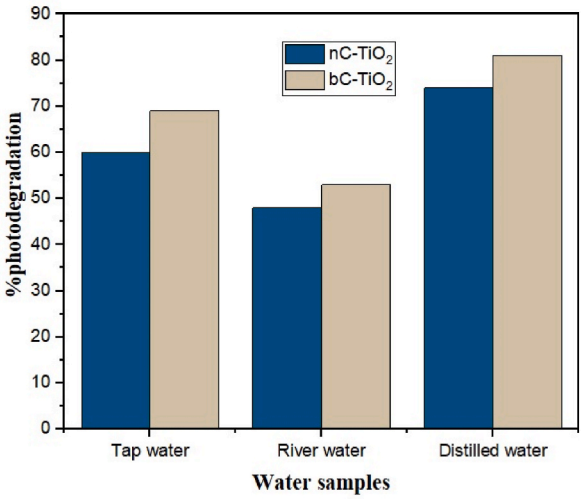

Fig. 15. Effect of real water samples.

4. Conclusion

The photocatalytic degradation of NFX under visible light was successfully demonstrated in this work. In this study, two samples of **C-TiO_2** photocatalyst (nanoparticles) were synthesized via the sol-gel method using n-hexane and benzene as precursors of carbon. The XRD result shows that both the samples of C-TiO_2 were of pure anatase phase. The SEM analysis indicates the spherical shape and nano size of the particles. The atomic% of carbon was 6.24 % in nC-TiO_2 and 7.98 % in bC-TiO_2. Both samples were employed for the degradation of NFX in the setup of visible radiation. The effect of irradiation time, catalyst dosage, initial concentration, and pH were investigated on the efficiency of the degradation. The result shows that the best photocatalytic performance (74 % & 81 %) was shown by both samples at pH 8 in 150 min. The catalyst dosage (10 mg for **nC-TiO_2** and 15 mg for **bC-TiO_2**) and concentration of NFX (10 ppm) were optimized. The kinetic study shows that the degradation of NFX follows pseudo-2nd -order kinetics with a rate constant (3.2×10^{-6} and 2.98×10^{-6} min^{-1}). From the degradation equilibrium study, it was found that the degradation of NFX follows the Langmuir adsorption isotherm which indicates the homogenous nature of **C-TiO_2** nanoparticles and monolayer adsorption of NFX on the surface of the photocatalyst. These results imply that **C-TiO_2** is a potentially useful photocatalyst for the effective removal of antibiotics, including NFX. Overall, this research highlights the potential of **C-TiO_2** addressing the rising problem of antibiotic contamination and advances the development of new photocatalytic materials for environmental remediation.

CRediT authorship contribution statement

Adnan: Writing – review & editing, Supervision, Project administration, Funding acquisition, Data curation, Conceptualization, Formal analysis, Methodology, Writing – original draft. **Kalsoom:** Writing – original draft, Validation, Methodology, Conceptualization, Data curation, Formal analysis. **Farah Muhammad Zada:** Data curation, Writing – review & editing. **Sarwat:** Data curation, Writing – review & editing. **Ho Soonmin:** Validation, Funding acquisition, Writing – review & editing. **Behramand Khan:** Data curation, Investigation, Validation, Writing – review & editing. **Muhammad Alamzeb:** Validation, Resources. **Wei Sun:** Writing – review & editing, Funding acquisition, Formal analysis. **Jawad Ikram:** Writing – review & editing. **Najeeb ur Rehman:** Resources.

Data and code availability statement

No data was used for the research described in the article.

Declaration of competing interest

The authors declare that they have no known competing financial interests or personal relationships that could have appeared to influence the work reported in this paper.

Acknowledgment

The authors acknowledge Institute of Chemical Sciences, University of Swat, for providing a conductive research environment and necessary resources.

References

[1] J. Zhang, D. Fu, J. Wu, Photodegradation of Norfloxacin in aqueous solution containing algae, J. Environ. Sci. (China) 24 (2012) 743–749, https://doi.org/10.1016/s1001-0742(11)60814-0.

[2] Z. Xu, X. Xue, S. Hu, Y. Li, J. Shen, Y. Lan, R. Zhou, F. Yang, C.J. Cheng, Degradation effect and mechanism of gas-liquid phase dielectric barrier discharge on norfloxacin combined with H2O2 or Fe2+, Separ. Purif. Technol. 230 (2020) 115862 https://doi.org/10.1016/j.seppur.2019.115862.

[3] L. Tang, J. Wang, G. Zeng, Y. Liu, Y. Deng, Y. Zhou, J. Tang, J. Wang, Z. Guo, Enhanced photocatalytic degradation of norfloxacin in aqueous Bi2WO6 dispersions containing nonionic surfactant under visible light irradiation, J. Hazard Mater. 306 (2016) 295–304, https://doi.org/10.1016/j.jhazmat.2015.12.044.

[4] M. Sayed, J.A. Khan, L.A. Shah, N.S. Shah, H.M. Khan, F. Rehman, A.R. Khan, A.M. Khan, Degradation of quinolone antibiotic, norfloxacin, in aqueous solution using gamma-ray irradiation, Environ. Sci. Pollut. Res. Int. 23 (2016) 13155–13168, https://doi.org/10.1007/s11356-016-6475-x.

[5] M. Sayed, L.A. Shah, J.A. Khan, N.S. Shah, J. Nisar, H.M. Khan, P. Zhang, A.R.J. Khan, Efficient photocatalytic degradation of norfloxacin in aqueous media by hydrothermally synthesized immobilized TiO2/Ti films with exposed {001} facets, J. Phys. Chem. 120 (2016) 9916–9931, https://doi.org/10.1021/acs.jpca.6b09719.

[6] H. Yang, L. Mei, P. Wang, J. Genereux, Y. Wang, B. Yi, C. Au, L. Dang, P.J. Feng, Photocatalytic degradation of norfloxacin on different TiO 2− X polymorphs under visible light in water, RSC Adv. 7 (2017) 45721–45732, https://doi.org/10.1039/C7RA09022F.

[7] J.-j. Wang, T. Lin, G.-m. Zeng, Y.-y. Zhou, Y.-c. Deng, C.-z. Fan, J.-l. Gong, Y.-n.J. Liu, Effect of bismuth tungstate with different hierarchical architectures on photocatalytic degradation of norfloxacin under visible light, Trans. Nonferrous Metals Soc. China 27 (2017) 1794–1803, https://doi.org/10.1016/S1003-6326(17)60202-4.

[8] W. Liao, V.K. Sharma, S. Xu, Q. Li, L. Wang, Microwave-enhanced photolysis of norfloxacin: kinetics, matrix effects, and degradation pathways, Int. J. Environ. Res. Publ. Health 14 (2017) 1564, https://doi.org/10.3390/ijerph14121564.

[9] V. Sharma, R.V. Kumar, K. Pakshirajan, G.J. Pugazhenthi, Integrated adsorption-membrane filtration process for antibiotic removal from aqueous solution, Powder Technol. 321 (2017) 259–269, https://doi.org/10.1016/j.powtec.2017.08.040.

[10] H. Yu, Z. Zhang, L. Zhang, H. Dong, H.J. Yu, Improved Norfloxacin degradation by urea precipitation Ti/SnO2–Sb anode under photo-electro catalysis and kinetics investigation by BP-neural-network-physical modeling, J. Clean. Prod. 280 (2021) 124412, https://doi.org/10.1016/j.jclepro.2020.124412.

[11] L. Zhou, N. Li, G. Owens, Z.J. Chen, Simultaneous removal of mixed contaminants, copper and norfloxacin, from aqueous solution by ZIF-8, Chem. Eng. J. 362 (2019) 628–637, https://doi.org/10.1016/j.cej.2019.01.068.

[12] W.-P. Low, W.-J. Lim, H.-P. Lee, N.A. Rahman, Removal of Copper, Chromium, and Nickel Ions from aqueous solution by using different pre-treated orange peel, IOP Conf. Ser. Earth Environ. Sci. 1205 (2023) 012013, https://doi.org/10.1088/1755-1315/1205/1/012013.

[13] M. Omer Adnan, B. Khan, I. Khan, M. Alamzeb, F.M. Zada, I. Ullah, R. Shah, M. Alqarni, J. Simal-Gandara, Equilibrium, kinetic and thermodynamic studies for the adsorption of metanil yellow using carbonized pistachio shell-magnetic nanoparticles, Water 14 (2022) 4139.

[14] G. Shankaraiah, S. Poodari, D. Bhagawan, V. Himabindu, S.J.D. Vidyavathi, Degradation of antibiotic norfloxacin in aqueous solution using advanced oxidation processes (AOPs)—a comparative study, Desalination Water Treat. 57 (2016) 27804–27815, https://doi.org/10.1080/19443994.2016.1176960.

[15] H. Chen, Z. Zhang, D. Hu, C. Chen, Y. Zhang, S. He, J.J. Wang, Catalytic ozonation of norfloxacin using Co3O4/C composite derived from ZIF-67 as catalyst, Chemosphere 265 (2021) 129047, https://doi.org/10.1016/j.chemosphere.2020.129047.

[16] Q. Zhang, H. Zhang, Q. Zhang, Q. Huang, Degradation of norfloxacin in aqueous solution by atmospheric-pressure non-thermal plasma: mechanism and degradation pathways, Chemosphere 210 (2018) 433–439, https://doi.org/10.1016/j.chemosphere.2018.07.035.

[17] X. Jin, X. Zhou, P. Sun, S. Lin, W. Cao, Z. Li, W. Liu, Photocatalytic degradation of norfloxacin using N-doped TiO(2): Optimization, mechanism, identification of intermediates and toxicity evaluation, Chemosphere 237 (2019) 124433, https://doi.org/10.1016/j.chemosphere.2019.124433.

[18] B.M.F. Jones, D. Maruthamani, V.J. Muthuraj, Construction of novel n-type semiconductor anchor on 2D honey comb like FeNbO4/RGO for visible light drive photocatalytic degradation of norfloxacin, J. Photochem. Photobiol. Chem. 400 (2020) 112712, https://doi.org/10.1016/j.jphotochem.2020.112712.

[19] X. Lv, D.Y. Yan, F.L.-Y. Lam, Y.H. Ng, S. Yin, A.K.J. An, Solvothermal synthesis of copper-doped BiOBr microflowers with enhanced adsorption and visible-light driven photocatalytic degradation of norfloxacin, Chem. Eng. J. 401 (2020) 126012, https://doi.org/10.1016/j.cej.2020.126012.

[20] H. Yu, F. Chen, L. Ye, H. Zhou, T.J. Zhao, Enhanced photocatalytic degradation of norfloxacin under visible light by immobilized and modified In2O3/TiO2 photocatalyst facilely synthesized by a novel polymeric precursor method, J. Mater. Sci. 54 (2019) 10191–10203, https://doi.org/10.1007/s10853-019-03636-z.

[21] D. Ding, C. Liu, Y. Ji, Q. Yang, L. Chen, C. Jiang, T.J. Cai, Mechanism insight of degradation of norfloxacin by magnetite nanoparticles activated persulfate: identification of radicals and degradation pathway, Chem. Eng. J. 308 (2017) 330–339, https://doi.org/10.1016/j.cej.2016.09.077.

[22] X. Ma, Y. Cheng, Y. Ge, H. Wu, Q. Li, N. Gao, J. Deng, Ultrasound-enhanced nanosized zero-valent copper activation of hydrogen peroxide for the degradation of norfloxacin, Ultrason. Sonochem. 40 (2018) 763–772, https://doi.org/10.1016/j.ultsonch.2017.08.025.

[23] H. Mohan, M. Ramasamy, V. Ramalingam, K. Natesan, M. Duraisamy, J. Venkatachalam, T. Shin, K.K. Seralathan, Enhanced visible light-driven photocatalysis of iron-oxide/titania composite: norfloxacin degradation mechanism and toxicity study, J. Hazard Mater. 412 (2021) 125330, https://doi.org/10.1016/j.jhazmat.2021.125330.

[24] D. Cao, Y. Wang, M. Qiao, X.J. Zhao, Enhanced photoelectrocatalytic degradation of norfloxacin by an Ag3PO4/BiVO4 electrode with low bias, J. Catal. 360 (2018) 240–249, https://doi.org/10.1016/j.jcat.2018.01.017.

[25] S. Lee, C.Y. Yun, M.S. Hahn, J. Lee, J.J. Yi, Synthesis and characterization of carbon-doped titania as a visible-light-sensitive photocatalyst, Kor. J. Chem. Eng. 25 (2008) 892–896, https://doi.org/10.1007/s11814-008-0147-6.

[26] R. Klaysri, M. Ratova, P. Praserthdam, P.J.J. Kelly, Deposition of visible light-active C-doped titania films via magnetron sputtering using CO2 as a source of carbon, Nanomaterials 7 (2017) 113, https://doi.org/10.3390/nano7050113.

[27] D. Chen, Z. Jiang, J. Geng, Q. Wang, D.J. Yang, Carbon and nitrogen co-doped TiO2 with enhanced visible-light photocatalytic activity, Ind. Eng. Chem. Res. 46 (2007) 2741–2746, https://doi.org/10.1021/ie061491k.

[28] M. Alsawat, T. Altalhi, K. Gulati, A. Santos, D.J. Losic, Synthesis of carbon nanotube–nanotubular titania composites by catalyst-free CVD process: insights into the formation mechanism and photocatalytic properties, ACS Appl. Mater. Interfaces 7 (2015) 28361–28368, https://doi.org/10.1021/acsami.5b08956.

[29] G. Jia, Y. Wang, X. Cui, W.J. Zheng, Highly carbon-doped TiO2 derived from MXene boosting the photocatalytic hydrogen evolution, ACS Sustain. Chem. Eng. 6 (2018) 13480–13486, https://doi.org/10.1021/acssuschemeng.8b03406.

[30] Y. Li, D.-S. Hwang, N.H. Lee, S.-J.J. Kim, Synthesis and characterization of carbon-doped titania as an artificial solar light sensitive photocatalyst, Chem. Phys. Lett. 404 (2005) 25–29, https://doi.org/10.1016/j.cplett.2005.01.062.

[31] M. Chen, W. Chu, Degradation of antibiotic norfloxacin in aqueous solution by visible-light-mediated C-TiO2 photocatalysis, J. Hazard Mater. 219–220 (2012) 183–189, https://doi.org/10.1016/j.jhazmat.2012.03.074.

[32] Z. Noorimotlagh, I. Kazeminezhad, N. Jaafarzadeh, M. Ahmadi, Z. Ramezani, S. Silva Martinez, The visible-light photodegradation of nonylphenol in the presence of carbon-doped TiO(2) with rutile/anatase ratio coated on GAC: effect of parameters and degradation mechanism, J. Hazard Mater. 350 (2018) 108–120, https://doi.org/10.1016/j.jhazmat.2018.02.022.

[33] J. Jia, D. Li, J. Wan, X.J. Yu, Characterization and mechanism analysis of graphite/C-doped TiO2 composite for enhanced photocatalytic performance, J. Ind. Eng. Chem. 33 (2016) 162–169, https://doi.org/10.1016/j.jiec.2015.09.030.

[34] S. Au–pree, P. Narakaew, S. Thungprasert, T. Promanan, A. Chaisena, S.J. Narakaew, Enhanced photocatalytic activity of C-doped TiO 2 under visible light irradiation: a Comparison of corn starch, honey, and polyethylene glycol as a carbon sources, Eng. J. 25 (2021) 53–68, https://doi.org/10.4186/ej.2021.25.1.53.

[35] M. Kamranifar, A. Allahresani, A. Naghizadeh, Synthesis and characterizations of a novel CoFe(2)O(4)@CuS magnetic nanocomposite and investigation of its efficiency for photocatalytic degradation of penicillin G antibiotic in simulated wastewater, J. Hazard Mater. 366 (2019) 545–555, https://doi.org/10.1016/j.jhazmat.2018.12.046.
[36] M. Malakootian, A. Nasiri, M.J. Amiri Gharaghani, Photocatalytic degradation of ciprofloxacin antibiotic by TiO2 nanoparticles immobilized on a glass plate, Chem. Eng. Commun. 207 (2020) 56–72, https://doi.org/10.1080/00986445.2019.1573168.
[37] A. Kumar, G.J. Pandey, A review on the factors affecting the photocatalytic degradation of hazardous materials, Mater. Sci. Eng. Int. J 1 (2017) 1–10, https://doi.org/10.15406/mseij.2017.01.00018.
[38] T.A. Gad-Allah, M.E. Ali, M.I. Badawy, Photocatalytic oxidation of ciprofloxacin under simulated sunlight, J. Hazard Mater. 186 (2011) 751–755, https://doi.org/10.1016/j.jhazmat.2010.11.066.
[39] P. Argurio, E. Fontananova, R. Molinari, E.J. Drioli, Photocatalytic membranes in photocatalytic membrane reactors, Processes 6 (2018) 162, https://doi.org/10.3390/pr6090162.
[40] S. Nekouei, F.J. Nekouei, Photocatalytic degradation of norfloxacin and its intermediate degradation products using nitrogen-doped activated carbon–CuS nanocomposite assisted by visible irradiation, Appl. Organomet. Chem. 32 (2018) e4418, https://doi.org/10.1002/aoc.4418.
[41] M. Chen, W.J. Chu, Degradation of antibiotic norfloxacin in aqueous solution by visible-light-mediated C-TiO2 photocatalysis, J. Hazard Mater. 219 (2012) 183–189, https://doi.org/10.1016/j.jhazmat.2012.03.074.
[42] S. Mortazavian, A. Saber, D.E.J. James, Optimization of photocatalytic degradation of acid blue 113 and acid red 88 textile dyes in a UV-C/TiO2 suspension system: application of response surface methodology (RSM), Catalysts 9 (2019) 360, https://doi.org/10.3390/catal9040360.
[43] S. Jafari, B. Yahyaei, E. Kusiak-Nejman, M.J. Sillanpää, The influence of carbonization temperature on the modification of TiO2 in the removal of methyl orange from aqueous solution by adsorption, Desalination Water Treat. 57 (2016) 18825–18835, https://doi.org/10.1080/19443994.2015.1094678.
[44] L.R. Gouvea, D.A. Martins, G. Batista Dda, N. Soeiro Mde, S.R. Louro, P.J. Barbeira, L.R. Teixeira, Norfloxacin Zn(II)-based complexes: acid base ionization constant determination, DNA and albumin binding properties and the biological effect against Trypanosoma cruzi, Biometals 26 (2013) 813–825, https://doi.org/10.1007/s10534-013-9661-z.
[45] F. Batool, J. Akbar, S. Iqbal, S. Noreen, S.N.A. Bukhari, Study of isothermal, kinetic, and thermodynamic parameters for adsorption of cadmium: an overview of linear and nonlinear approach and error analysis, Bioinorgan. Chem. Appl. 2018 (2018) 3463724, https://doi.org/10.1155/2018/3463724.
[46] T.S. Khayyun, A.H.J. Mseer, Comparison of the experimental results with the Langmuir and Freundlich models for copper removal on limestone adsorbent, Appl. Water Sci. 9 (2019) 170, https://doi.org/10.1007/s13201-019-1061-2.
[47] B.H. Hameed, A.T. Din, A.L. Ahmad, Adsorption of methylene blue onto bamboo-based activated carbon: kinetics and equilibrium studies, J. Hazard Mater. 141 (2007) 819–825, https://doi.org/10.1016/j.jhazmat.2006.07.049.
[48] M. Chen, W.J. Chu, Photocatalytic degradation and decomposition mechanism of fluoroquinolones norfloxacin over bismuth tungstate: experiment and mathematic model, Appl. Catal. B Environ. 168 (2015) 175–182, https://doi.org/10.1016/j.apcatb.2014.12.023.
[49] X. Chen, J.J. Wang, Degradation of norfloxacin in aqueous solution by ionizing irradiation: kinetics, pathway and biological toxicity, Chem. Eng. J. 395 (2020) 125095, https://doi.org/10.1016/j.cej.2020.125095.
[50] L. Fang, K. Tang, D. Wei, Y. Zhang, Y. Zhou, Photocatalytic degradation of norfloxacin by magnetic molecularly imprinted polymers: influencing factors and mechanisms, Environ. Technol. 44 (2023) 1438–1449, https://doi.org/10.1080/09593330.2021.2003442.